ELSEVIER

21 September 2000

Physics Letters B 489 (2000) 287–292

PHYSICS LETTERS B

www.elsevier.nl/locate/npe

Tilted pion sources from azimuthally sensitive HBT interferometry

Michael Annan Lisa [a], Ulrich Heinz [b], Urs Achim Wiedemann [b]

[a] *Department of Physics, The Ohio State University, 174 W. 18th Avenue, Columbus, OH 43210, USA*
[b] *Theoretical Physics Division, CERN, CH-1211 Geneva 23, Switzerland*

Received 15 July 2000; accepted 16 August 2000
Editor: P.V. Landshoff

Abstract

Intensity interferometry in noncentral heavy ion collisions provides access to novel information on the geometry of the effective pion-emitting source. We demonstrate analytically that, even for vanishing pair momentum, the cross terms R_{ol}^2 and R_{sl}^2 of the HBT correlation function in general show a strong first harmonic in their azimuthal dependence. The strength of this oscillation characterizes the tilt of the major axis of the spatial emission ellipsoid away from the direction of the beam. Event generator studies indicate that this tilt can be large ($> 20°$) at AGS energies which makes it by far the most significant azimuthally sensitive HBT signal at these energies. Moreover, transport models suggest that for pions this spatial tilt is directed *opposite* to the tilt of the directed flow ellipsoid in momentum space. A measurement of the azimuthal dependence of the HBT cross terms R_{ol}^2 and R_{sl}^2 thus probes directly the physical origin of directed pion flow.

PACS: 25.75.+r; 07.60.ly; 52.60.+h

Two-particle momentum correlations between identical particles are commonly used to extract space-time and dynamical information about the particle emitting source in heavy ion collisions. The basis for this intensity interferometric method is the equation [1–3]

$$C(\boldsymbol{q},\boldsymbol{K}) = 1 + \frac{\left|\int d^4x\, S(x,K)\, e^{iq\cdot x}\right|^2}{\left|\int d^4x\, S(x,K)\right|^2}, \qquad (1)$$

$q = p_1 - p_2$, $K = \frac{1}{2}(p_1 + p_2)$, which relates the phase-space density $S(x,K)$ of the source to the measured 2-particle correlation function $C(\boldsymbol{q},\boldsymbol{K})$. Experimental measurements of C are usually parametrized in terms of the intercept $\lambda(\boldsymbol{K})$ and the HBT radii $R_{ij}^2(\boldsymbol{K})$ by

$$C(\boldsymbol{q},\boldsymbol{K}) = 1 + \lambda(\boldsymbol{K}) \times \exp\left[-\sum_{i,j=o,s,l} q_i q_j R_{ij}^2(\boldsymbol{K})\right]. \qquad (2)$$

In this Cartesian *osl*-system the relative momentum is decomposed into components parallel to the beam (l = *longitudinal*), parallel to the transverse component of $\boldsymbol{K}$ (o = *out*), and in the remaining third direction (s = *side*).

Over the last decade the experimental frontier in studying identical two-particle correlations was defined by more and more differential measurements of

0370-2693/00/$ - see front matter
PII: S0370-2693(00)00952-7

the HBT radii $R_{ij}^2(\boldsymbol{K})$. At both AGS [4,5] and SPS [6] energies, the longitudinal (K_L) and transverse ($K_\perp$) pair momentum dependence is now well-studied for central and reaction-plane averaged non-central collisions. Most importantly, these studies have led to a detailed characterization of the longitudinal expansion and the transverse radial flow of the reaction zone. The next challenge is a similarly detailed study of the $R_{ij}^2(\boldsymbol{K})$ as a function of the azimuthal orientation Φ of the transverse pair momentum $\boldsymbol{K}_\perp$ with respect to the impact parameter $\boldsymbol{b}$ in non-central collisions. This Φ-dependence reveals qualitatively new information about the space-time structure of the source and yields new insights on the underlying nature of flow. In fact, under reasonable assumptions *all 10 components of the source's spatial correlation tensor can be recovered.*

An azimuthally sensitive HBT analysis involves all six parameters R_{ij}^2, all of which are functions of all 3 components of the pair momentum $K_\perp$, Y and Φ[1]. They provide information about the source in space-time according to the following relations [3,7]:

$$\begin{aligned}
R_s^2(K_\perp,\Phi,Y) &= S_{11}\sin^2\Phi + S_{22}\cos^2\Phi \\
&\quad - S_{12}\sin 2\Phi\,, \\
R_o^2(K_\perp,\Phi,Y) &= S_{11}\cos^2\Phi + S_{22}\sin^2\Phi + S_{12}\sin 2\Phi \\
&\quad - 2\beta_\perp S_{01}\cos\Phi - 2\beta_\perp S_{02}\sin\Phi \\
&\quad + \beta_\perp^2 S_{00}\,, \\
R_{os}^2(K_\perp,\Phi,Y) &= S_{12}\cos 2\Phi + \tfrac{1}{2}(S_{22}-S_{11})\sin 2\Phi \\
&\quad + \beta_\perp S_{01}\sin\Phi - \beta_\perp S_{02}\cos\Phi\,, \\
R_l^2(K_\perp,\Phi,Y) &= S_{33} - 2\beta_l S_{03} + \beta_l^2 S_{00}\,, \\
R_{ol}^2(K_\perp,\Phi,Y) &= (S_{13}-\beta_l S_{01})\cos\Phi - \beta_\perp S_{03} \\
&\quad + (S_{23}-\beta_l S_{02})\sin\Phi \\
&\quad + \beta_l\beta_\perp S_{00}\,, \\
R_{sl}^2(K_\perp,\Phi,Y) &= (S_{23}-\beta_l S_{02})\cos\Phi \\
&\quad - (S_{13}-\beta_l S_{01})\sin\Phi\,. \qquad (3)
\end{aligned}$$

The pair velocity $\boldsymbol{\beta} = \boldsymbol{K}/K^0$ arises from the on-shell constraint [3] $q^0 = \boldsymbol{q}\cdot\boldsymbol{\beta}$; it mixes spatial and temporal information. $S_{\mu\nu}$ denotes the spatial correlation tensor

$$S_{\mu\nu} = \langle \tilde{x}_\mu \tilde{x}_\nu \rangle\,, \quad \tilde{x}_\mu = x_\mu - \bar{x}_\mu\,, \quad (\mu,\nu = 0,1,2,3) \qquad (4)$$

which measures the Gaussian width in space-time of the emission function $S(x,K)$ around the point of highest emissivity $\bar{x}_\mu = \langle \tilde{x}_\mu \rangle$ [3]:

$$\langle \tilde{x}_\mu \tilde{x}_\nu \rangle(K) = \frac{\int d^4x\, \tilde{x}_\mu \tilde{x}_\nu\, S(x,K)}{\int d^4x\, S(x,K)}\,. \qquad (5)$$

It is the inverse of the curvature tensor $B_{\mu\nu}$ [8]:

$$S(x,K) \approx N(K)\, S(\bar{x},K) \exp\Big[-\tfrac{1}{2}\tilde{x}^\mu B_{\mu\nu}\tilde{x}^\nu\Big]\,. \qquad (6)$$

This approximation neglects non-Gaussian components of the emission function whose influence on the HBT radii can in most practical cases be neglected [3]. We emphasize that in (4) $S_{\mu\nu}$ is defined in terms of Cartesian coordinates in an impact parameter fixed system, in which $x_1 = x$ is parallel to the impact parameter $\boldsymbol{b}$ and $x_3 = z$ lies in the beam direction.

The general relations (3) separate the *explicit* Φ-dependence of the HBT-radii (which is a consequence of the azimuthal rotation of the *osl*-system relative to (x_1,x_2,x_3)) from the *implicit* Φ-dependence of the space-time widths $\langle \tilde{x}_\mu \tilde{x}_\nu \rangle(K_\perp,Y,\Phi)$ (which reflects a Φ-dependent change of the shape of the effective emission region) [7]. Existing studies of (3) focussed on the detailed interplay between explicit and implicit Φ-dependences in the HBT radii R_s^2, R_o^2 and R_{os}^2 [7,9,10]. Here we show, however, that some of the most striking features are found in analyzing the Φ-dependences of R_{ol}^2 and R_{sl}^2 which so far received less attention [9].

The following discussion is simplified significantly by the important observation that the implicit Φ-dependence of $S_{\mu\nu}$ is weak. It can be neglected relative to the explicit one given in (3) as long as the Φ-dependence of space-momentum correlations in the source is small compared to the thermal smearing, and for $K_\perp \to 0$ it vanishes completely. Studies with the RQMD model [11] indicate that the first

[1] For central collisions 4 radius parameters depending only on Y and $K_\perp$ suffice [3]

condition works well at least up to $p_T = 300$ MeV/c for Au + Au collisions at 2 AGeV [12]. Beyond such model studies, a simple scale argument illustrates why neglecting the implicit Φ-dependence relative to the explicit one has a much wider kinematical region of validity than neglecting the implicit $K_\perp$-dependence relative to the explicit one in (3): the latter is suppressed near $K_\perp = 0$ ($\beta_\perp = 0$), and it multiplies only space-time variances involving $\tilde{t}$ which are numerically small in practice. In contrast, the explicit Φ-dependence in (3) leads to prefactors $\cos(n\Phi)$, $\sin(n\Phi)$ oscillating between 1 and -1 even for $K_\perp = 0$, and it multiplies the numerically large components of $S_{\mu\nu}$. The assumption of vanishing implicit Φ-dependence can be checked experimentally [7], and deviations can be quantified in a full harmonic analysis given elsewhere [7,12]. Also, while it requires weak *transverse* flow, there is no such restriction on the longitudinal flow. Qualitatively, the main findings presented here do not depend on this assumption, but it simplifies our presentation and allows for a particularly intuitive geometric picture of the new effect discussed here.

With this proviso, the components $S_{\mu\nu}$ in (3) become Φ-independent constants which describe the *same* source being viewed from all angles Φ. We turn briefly to symmetry considerations at midrapidity. Considering collisions between equal mass nuclei, it can be rigorously shown [12] that, as a consequence of point reflection symmetry around the spatial origin and mirror symmetry with respect to the reaction plane, five of the off-diagonal components $S_{\mu\nu}$ (all except S_{13}) oscillate symmetrically around zero. Coupled with the condition of vanishing implicit Φ-dependence this implies

$$S_{01} = 0\,, \quad S_{02} = 0\,, \quad S_{03} = 0\,, \quad S_{12} = 0\,, \quad S_{23} = 0\,. \tag{7}$$

These equations and the fact that around midrapidity the average β_l is zero (although average $\beta_l^2 \neq 0$) allow us to write the HBT radius parameters (3) in terms of 5 non-vanishing components only:

$$\begin{aligned}
&R_s^2 = \tfrac{1}{2}(S_{11} + S_{22}) + \tfrac{1}{2}(S_{22} - S_{11})\cos 2\Phi\,,\\
&R_o^2 = \tfrac{1}{2}(S_{11} + S_{22}) - \tfrac{1}{2}(S_{22} - S_{11})\cos 2\Phi + \beta_\perp^2 S_{00}\,,\\
&R_{os}^2 = \tfrac{1}{2}(S_{22} - S_{11})\sin 2\Phi \quad R_l^2 = S_{33} + \beta_l^2 S_{00}\,,\\
&R_{ol}^2 = S_{13}\cos\Phi\,, \quad R_{sl}^2 = -S_{13}\sin\Phi\,.
\end{aligned} \tag{8}$$

Since the Φ-dependences of R_s^2 and R_o^2 explicitly separate S_{22} from S_{11}, the emission duration S_{00} can now be determined without additional model assumptions [3,10], contrary to the case of collisions at $b = 0$.

Given the measured weak Y-dependence of the HBT-radii [3–6], Eqs. (8) can be used in practice also for event samples which are averaged over large Y-windows symmetric around $Y = 0$. According to (8), the HBT radius parameters R_o^2, R_s^2 and R_{os}^2 all show second harmonic oscillations of the same strength $\frac{1}{2}(S_{11} - S_{22})$. This is the $R_{o,2}^{c\,2} = -R_{s,2}^{c\,2} = -R_{os,2}^{s\,2}$ rule for second harmonic coefficients [7]; leading deviations from this rule have been quantified [7,12] and provide a consistency check on the assumption of negligible implicit Φ-dependence. More strikingly, R_{ol}^2 and R_{sl}^2 display purely *first harmonic oscillation at midrapidity* which are easier to measure. The expected identical amplitudes for these oscillations provide a further consistency check on our assumptions.

The required Φ-binning puts severe demands on the pair statistics. A first observation of azimuthally oscillating HBT radii was reported in [13]. Such measurements require a reasonably accurate determination of the reaction plane; a typical uncertainty of 30° reduces the first and second harmonics in (3) by $\sim 15\%$ and $\sim 45\%$, respectively, but these losses can be corrected for [7,14].

While the amplitude of the oscillations of R_o^2, R_s^2, and R_{os}^2 are given by the difference between the transverse source sizes in and perpendicular to the reaction plane, that of the oscillations of R_{sl}^2 and R_{ol}^2 is given by $S_{13} \equiv \langle \tilde{x}\tilde{z} \rangle$. Parameterizing the source by an ellipsoid, a nonzero S_{13} corresponds to a tilt in the reaction plane of the longitudinal major axis of the ellipsoid away from the beam direction. It can be characterized by a tilt angle

$$\theta_s = \tfrac{1}{2}\tan^{-1}\left(\frac{2S_{13}}{S_{33} - S_{11}}\right). \tag{9}$$

Rotating the spatial correlation tensor $S_{\mu\nu}$ by θ_s yields a purely diagonal tensor $S' = R_y^\dagger(\theta_s) \cdot S \cdot R_y(\theta_s)$ whose eigenvalues are the squared lengths of the 3 major axes.

We illustrate the role of the tilt angle (9) with a tilted Gaussian toy distribution with no space-momentum correlations:

$$S(x,K) = e^{-E/T}\exp\left(-\frac{x'^2}{2\sigma_x^2} - \frac{y^2}{2\sigma_y^2} - \frac{z'^2}{2\sigma_z^2} - \frac{t^2}{2\sigma_t^2}\right),$$

$$x' = x\cos\Theta - z\sin\Theta, \quad z' = x\sin\Theta + z\cos\Theta. \quad (10)$$

To avoid relativistic complications, the 'temperature' T is kept small (20 MeV) in the following. Fig. 1 shows the projection of this source onto the reaction (xz) plane.

Using the model (10) with the parameters of Fig. 1 to randomly generate a set of phase-space points, we constructed a three-dimensional correlation function (with $\approx 4\times10^5$ pairs with $q < 100$ MeV/c) for each of eight 45°-wide Φ bins, according to the prescription and code of Pratt [15]. Fitting each with the Gaussian parametrization (2) yields the HBT radii presented in Fig. 2. Treating the ten components of $S_{\mu\nu}$ as parameters, we perform a global fit with Eqs. (3) on these Φ-dependent radii. The fit results are indicated by solid lines in Fig. 2. Application of (9) to the fit results yields $\theta_s = 24.6° \pm 0.6°$, in good agreement with the input value $\Theta = 25°$. The diagonal elements $S'_{\mu\mu}$ reproduce, within statistical errors, the input values for the squares of the homogeneity lengths: $\sigma_x = 4.05 \pm 0.05$ fm, $\sigma_y = 4.97 \pm 0.04$ fm, $\sigma_z = 6.97 \pm 0.04$ fm, and $\sigma_t = 4.78 \pm 0.45$ fm. (The larger uncertainty in σ_t arises from the low $\beta_\perp$ of the pions in our example.)

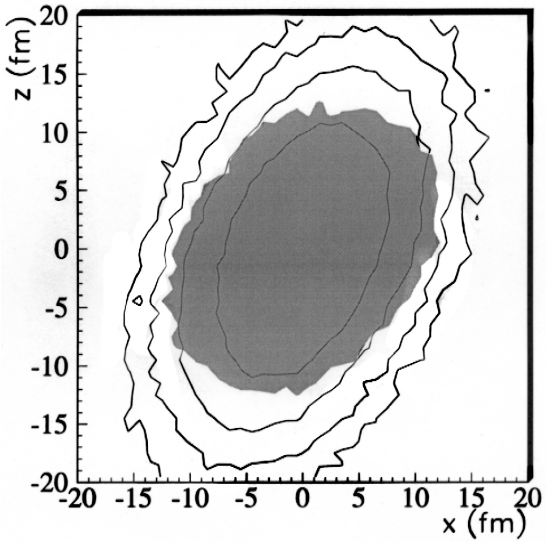

Fig. 1. The tilt of the spatial distribution of pion emission points projected onto the reaction (xz) plane. Contours show on a logarithmic scale the spatial distribution for the toy model (10) with $\sigma_t = 5\,\text{fm}/c$, $\sigma_x = 4\,\text{fm}$, $\sigma_y = 5\,\text{fm}$, $\sigma_z = 7\,\text{fm}$, and $\Theta = 25°$. The shaded region is the distribution of emission points of pions with $|p_z| < 40$ MeV/c in the toy model including longitudinal flow. See text for details.

While one may escape the effects of transverse flow (which may generate a Φ-dependent effective source) by selecting pion pairs at low $K_\perp$, longitudinal flow, which generates $z - p_z$ correlations, is generally stronger and cannot be cut away. Fortunately, since they are essentially orthogonal to the azimuthal dependences we are discussing, such correlations do not drastically alter the intuitive geometric picture we have discussed – the same source is still viewed from all angles Φ.

As an example we added a boost-invariant longitudinal flow component in z-direction to our toy source (scaled so that the collective flow velocity at $z = \pm\sigma_z$ is equal to the thermal velocity), leaving the geometry unchanged. This results in (i) an increase in the tilt angle θ_s from 25° to 33° and (ii) a reduction in S'_{33} from 49 fm^2 to 31 fm^2. The other components $S'_{\mu\mu}$ vary negligibly from the scenario without flow. Familiar from the case of azimuthally symmetric HBT, effect (ii) is understood in terms of a reduction in the length of homogeneity due to the flow [3]: HBT correlations arise from particle pairs with close-by momenta; the space-momentum correlations induced by longitudinal flow then imply that they will be close-by in coordinate space as well. The increased tilt is similarly understood, by examining the spatial distribution of emission points for pions with low p_z. The shaded region in Fig. 1 shows the effective source for pions with $|p_z| < 40$ MeV/c; it is clearly less prolate and more tilted than in the case of no flow (contour lines).

Φ-sensitive HBT studies and the measurement of spatial tilt connect for the first time the physics of directed flow with the space-time structure of the source [9]. We consider this an essential step towards a full understanding of the phase-space dynamics of

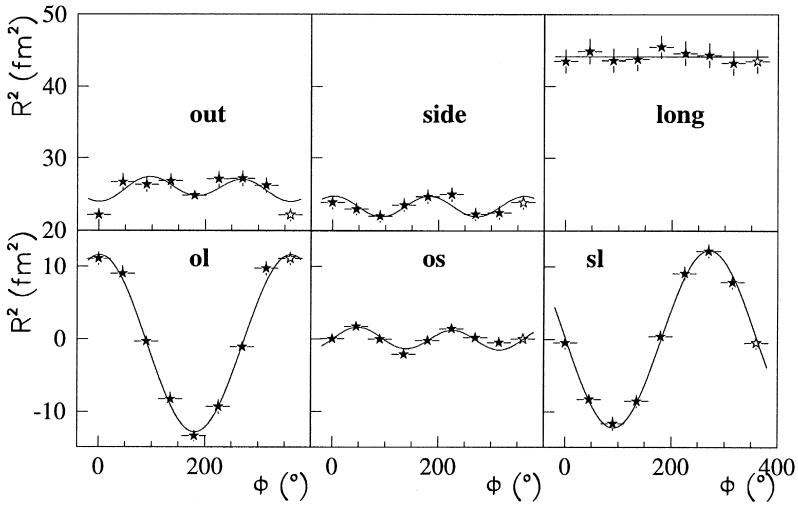

Fig. 2. Azimuthal dependence of the HBT radii from fits to correlation functions generated from the toy source (10). Solid lines represent a global fit to $R(\Phi)$ with (3). The value from $\Phi = 0°$ is replotted with an open symbol at $\Phi = 360°$.

heavy-ion collisions. Although a detailed discussion must await a longer paper, we here shortly touch on the main physics points, using results from a realistic transport model.

We performed simulations of semiperipheral Au + Au collisions at 2 AGeV with the RQMD (v2.3) model [11]. The top panel of Fig. 3 shows $\langle p_x \rangle$ – the average pion momentum in the reaction plane – as a function of momentum p_z along the beam axis. Qualitatively consistent with experimental observations [16], a very weak negative directed flow ('anti-flow') signal is observed – the average emission ellipsoid in *momentum* space is tilted to a negative angle with respect to the beam (the direction of directed proton flow defines the positive direction). The magnitude of the collective motion ($\sim 10\,\mathrm{MeV}/c$) is small compared to the typical p_T scale ($\sim 200\,\mathrm{MeV}/c$); hence thermal smearing dominates. The bottom panel shows that, while the spatial distribution displays a richer structure than our toy model, it is nevertheless always characterized by a significant *positive* tilt – *opposite* the average tilt in momentum space. A full correlation function analysis of the RQMD events [12] yields qualitatively similar results as those shown in Fig. 2.

This bears directly on the physical causes of directed pion flow at these energies. Detailed transport model studies [17] have shown that pion reflection from (not absorption by) the nucleonic matter is

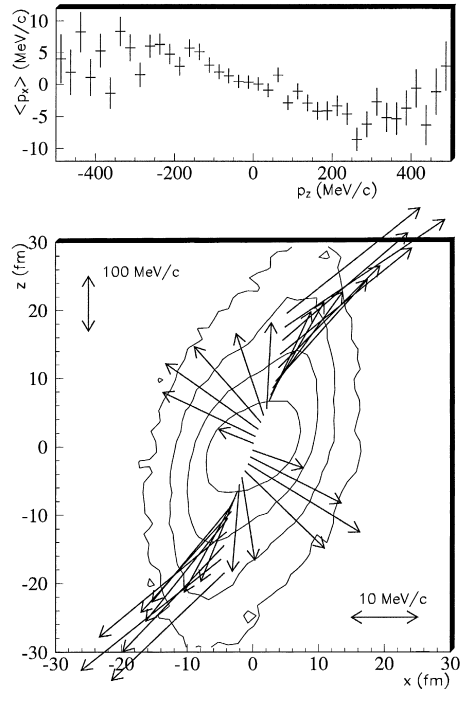

Fig. 3. RQMD simulation of pions from 2 AGeV Au + Au collisions at $b = 3$–7 fm. The top panel shows a weak $p_x - p_z$ 'anti-flow' correlation. In the bottom panel, contours of the spatial distribution of emission points projected onto the reaction plane show a strong tilt in the *opposite direction from the tilt in momentum space*. Superimposed arrows represent the average pion momentum at different values of z. Note that the momentum scale in z-direction is compressed for clarity.

at the root of directed pion flow at these energies. Focussing on the forward hemisphere, if absorption processes ($\pi NN \to \Delta N \to NN$) were dominant in producing pion flow, we would expect an absence of π emission points in the $+x$ quadrant, i.e. a negative tilt in coordinate space *and* in momentum space. Since it is the point of last scattering (as opposed to the original point of creation) which is relevant for HBT correlations [3], it is clear that reflection ($\pi N \to \Delta \to \pi N$) from flowing participant or spectator baryons leads to a positive tilt in coordinate space as seen in Fig. 3: the reflected pions 'illuminate' the coordinate-space anisotropies of the nucleonic matter. In this simple picture, then, the sign of θ_s immediately distinguishes between these two possibilities.

The arrows in Fig. 3 represent the average momenta of pions for different values of z. The resulting structure further underscores the importance of pion rescattering: Clearly, the more numerous pions from the high-density region around $z = 0$ dominate, generating the anti-flow signal seen in experiment. However, pions from the more dilute large-$|z|$ region have less opportunity for rescattering and so retain the *positive* $p_x - p_z$ correlation of their (flowing) parent Δ's. Similar considerations generate a sign change in the pion flow as the impact parameter is varied in transport models [17].

In summary, for non-central collisions all ten components of the spatial correlation tensor $S_{\mu\nu}$ are accessible by Φ-dependent HBT measurements. Based on symmetry and scale considerations we argue that for low $K_\perp$ the explicit Φ-dependence of Eqs. (3) dominates. Consistency relations allow to check whether this is true in practice. The spatial correlation tensor $S_{\mu\nu}$ can then be extracted completely from a global fit to the six Φ-dependent HBT radii. At midrapidity, the five nonvanishing components of $S_{\mu\nu}$ correspond to the four spacetime lengths of homogeneity and a tilt of the source in the reaction plane, away from the beam direction. This tilt, which may be quite large at AGS energies, causes striking and relatively easily measurable first-order harmonic oscillations in R_{ol} and R_{sl} and can give a direct experimental handle on the origin of pion flow at these energies.

Acknowledgements

The work of M.A.L. is supported by NSF Grant PHY-9722653 and that of U.H. by DFG, GSI and BMBF.

References

[1] E. Shuryak, Phys. Lett. B 44 (1973) 387; Sov. J. Nucl. Phys. 18 (1974) 667.
[2] S. Chapman, U. Heinz, Phys. Lett. B 340 (1994) 250.
[3] U.A. Wiedemann, U. Heinz, Phys. Rep. 319 (1999) 145.
[4] E877 Collaboration, J. Barrette et al., Phys. Rev. Lett. 78 (1997) 2916.
[5] E895 Collaboration, M.A. Lisa et al., Phys. Rev. Lett. 84 (2000) 2798.
[6] NA49 Collaboration, H. Appelshäuser et al., Eur. Phys. J. C 2 (1998) 661.
[7] U.A. Wiedemann, Phys. Rev. C 57 (1998) 266.
[8] S. Chapman, J.R. Nix, U. Heinz, Phys. Rev. C 52 (1995) 2694.
[9] S.A. Voloshin, W.E. Cleland, Phys. Rev. C 53 (1996) 896; Phys. Rev. C 54 (1996) 3212.
[10] H. Heiselberg, Phys. Rev. Lett. 82 (1999) 2052; H. Heiselberg, A.-M. Levy, Phys. Rev. C 59 (1999) 2716.
[11] H. Sorge, Phys. Rev. C 52 (1995) 3291.
[12] M.A. Lisa, U. Heinz, U.A. Wiedemann, work in progress.
[13] E895 Collaboration, M.A. Lisa et al., Nucl. Phys. A 661 (1999) 444c.
[14] S.A. Voloshin, Y. Zhang, Z. Phys. C 70 (1996) 665.
[15] S. Pratt, Nucl. Phys. A 566 (1993) 103c.
[16] EOS Collaboration, J. Kintner et al., Phys. Rev. Lett. 78 (1997) 4165.
[17] S.A. Bass et al., Phys. Lett. B 302 (1993) 381; Phys. Rev. C 51 (1995) 3343.